Combustion and Flame 235 (2022) 111691

Contents lists available at ScienceDirect

Combustion and Flame

journal homepage: www.elsevier.com/locate/combustflame

Interaction of NH_3 and NO under combustion conditions. Experimental flow reactor study and kinetic modeling simulation

M.U. Alzueta, L. Ara, V.D. Mercader, M. Delogu, R. Bilbao

Aragón Institute of Engineering Research (I3A), Department of Chemical and Environmental Engineering, University of Zaragoza, Zaragoza 50018, Spain

ARTICLE INFO

Article history:
Received 6 May 2021
Revised 10 August 2021
Accepted 11 August 2021
Available online 30 August 2021

Keywords:
Ammonia
Nitric oxide
NH_3-NO interaction
Kinetic modeling
Carbon-free fuel

ABSTRACT

The interaction between ammonia and NO under combustion conditions is analyzed in the present work, from both experimental and kinetic modelling points of view. An experimental systematic study of the influence of the main variables for the NH_3–NO interaction is made using a laboratory tubular flow reactor installation. Experiments are performed at atmospheric pressure and variables analyzed include: temperature in the 700–1500 K range, air stoichiometry, from pyrolysis to very oxidizing conditions, and the NH_3/NO ratio, in the 0.7–3.5 range. Nitrogen and argon have been used as diluent gas. A literature reaction mechanism has been used to simulate the present experimental results and discuss the main findings. Reaction path analysis has allowed the identification of the reaction routes under the studied conditions. The simulations reflect the main experimental trends observed. Main results show that NO reduction by NH_3 occurs at any conditions studied, but is more intense under oxygen excess conditions. Interactions of NH_3 and NO proceeds in a molar basis with optimum conversions of NO of up to almost 100%.

© 2021 The Authors. Published by Elsevier Inc. on behalf of The Combustion Institute.
This is an open access article under the CC BY-NC-ND license
(http://creativecommons.org/licenses/by-nc-nd/4.0/)

1. Introduction

Ammonia conversion under combustion conditions has become a major topic of research nowadays, mainly because of its interest as a carbon free fuel [1–10]. The use of ammonia implies both advantages and disadvantages. Among those, pollutants formation can be a major drawback. Combustion of ammonia produces ideally N_2 and water vapor as reaction products, but in practice formation of nitrogen oxides, NO in particular, can happen if high oxygen concentrations are available at the high temperatures of combustion, as found in ammonia oxidation studies (e.g., [5,6,11–13]. Even though there is still necessity for further studies dealing with the emission of NO_x and unburned NH_3, as is pointed out by Shu et al. [3], it is clear that formation of NO can occur during ammonia oxidation, and thus it is probable that both NH_3 and NO can be present together within the combustion chamber in a variety of conditions. If this happens, it is clear that mechanisms and strategies that imply a minimization of NO emissions must be implemented in real combustors fueled with ammonia. Therefore, it is compulsory to progress in the understanding of the interactions between NH3 and NO for ammonia combustors to be competitive.

The interaction of NH_3 and NO has been studied in the past mainly in works dealing with selective non-catalytic reduction (SNCR) of nitric oxides (e.g. [14–17], where ammonia or, in general selective nitrogen agents, are made to interact with NO under oxidizing conditions in a given temperature interval around 1250 K, the so-called temperature window of the SNCR process. Under those fuel-lean conditions, ammonia has demonstrated to react with NO, converting it to N_2, according to the following dominant mechanism:

$$NH_3+OH \rightleftharpoons NH_2+H_2O \quad (r1)$$

$$NH_2+NO \rightleftharpoons N_2+ H_2O \quad (r2)$$

where the NH_2 radicals formed from ammonia (mainly abstracted by OH as in reaction r1) can react selectively with NO to reduce it to molecular nitrogen, but can also get oxidized to NO, through:

$$NH_2+O_2 \rightleftharpoons NO+H_2O \quad (r3)$$

The competition between reactions 2 and 3 is driven by the specific environment in the reaction zone, and it can lead to a decrease of NO (r2) or an increase of it (r3).

While the interaction of ammonia and nitric oxide has been mainly considered in oxygen excess environments, the new scenario of using ammonia as a fuel requires as well the study of conditions with oxygen shortage. In this regard, studies are more

https://doi.org/10.1016/j.combustflame.2021.111691
0010-2180/© 2021 The Authors. Published by Elsevier Inc. on behalf of The Combustion Institute. This is an open access article under the CC BY-NC-ND license (http://creativecommons.org/licenses/by-nc-nd/4.0/)

Table 1
Matrix of experimental conditions. All experiments are performed at atmospheric pressure, with a total flow rate of around 1 L (STP)/min and using N_2 or Ar as diluent. The air excess ratio (λ) is determined considering the stoichiometry of reaction: $NH_3 + 0.75\ O_2 \rightleftharpoons 0.5\ N_2 + 1.5\ H_2O$.

Set	NH_3 (ppm)	NO (ppm)	NH_3/NO	O_2 (ppm)	H_2O (ppm)	Bath gas	λ	t_r (s)
1	1031	1006	1.02	0	0	N_2	0	195/T(K)
2	1066	1012	1.05	345	0	N_2	0.43	195/T(K)
3	1060	1003	1.06	435	0	N_2	0.55	195/T(K)
4	1015	1016	1.00	773	0	N_2	1.01	195/T(K)
4R	1013	1013	1.00	764	0	N_2	1.01	195/T(K)
5	1019	1006	1.01	784	5000	N_2	1.02	195/T(K)
6	1049	1002	1.05	1296	0	N_2	1.65	195/T(K)
7	1051	999	1.05	3820	0	N_2	4.85	195/T(K)
8	1044	300	3.48	1320	0	N_2	1.69	195/T(K))
9	1042	1520	0.68	1345	0	N_2	1.72	195/T(K)
10	1009	297	3.40	3834	0	N_2	5.07	195/T(K)
11	1028	1519	0.68	3814	0	N_2	4.95	195/T(K)
12	1012	1021	0.99	378	0	Ar	0.49	195/T(K)
13	1048	1110	0.94	675	0	Ar	0.86	179/T(K)
14	1010	1011	1.00	750	0	Ar	0.99	195/T(K)
15	1001	1030	0.97	880	0	Ar	1.17	195/T(K)
16	970	1075	0.90	1146	0	Ar	1.57	178/T(K)
17	898	1019	0.88	1530	0	Ar	2.27	180/T(K)
18	997	982	1.01	4100	0	Ar	5.48	182/T(K)
19	1013	315	3.22	750	0	Ar	0.99	195/T(K)
20	993	1526	0.65	750	0	Ar	1.01	195/T(K)
21	940	310	3.03	1600	0	Ar	2.27	180/T(K)
22	975	1425	0.68	1650	0	Ar	2.26	180/T(K)
23	954	302	3.16	4100	0	Ar	5.73	179/T(K)
24	938	1560	0.60	4100	0	Ar	5.83	245/T(K)

scarce, including, for instance, the works of Barbas et al. [12] and Mei et al. [18] in flames or the work of Dagaut [19], which faces NO and NH_3 sensitization effects in a jet-stirred-reactor (JSR) study. In this context, the present work addresses the interaction of NH_3 and NO under carefully controlled laboratory conditions, analyzing the effect of air stoichiometry and temperature, but also the NH_3/NO ratio. Additionally, the experiments made in the present work include the evaluation of water presence, and the use of two different diluents (nitrogen and argon). Experiments are interpreted in terms of a detailed kinetic model, and discussion of the main results attained is presented.

2. Experimental methodology

The experiments are performed at atmospheric pressure in an experimental installation previously used by the group to study the gas-phase oxidation process of different compounds, where a full description of it can be found (e.g. [11,20–22]). A brief description of it follows below.

Reactants (NH_3, NO, and O_2, diluted either in nitrogen or argon), and nitrogen or argon to balance, are fed from gas cylinders through mass flow controllers. Experiments with N_2 would be representative of real conditions of combustion systems, while experiments with Ar allow the quantification of N_2 formed from ammonia, and therefore the performance of N balances. In experiments where water was added, it was fed by saturating a nitrogen or argon stream in water. Following the procedure of Alzueta et al. [23], the gases are fed to the quartz tubular flow reactor in four separate streams, and mixed at the inlet of the reaction zone. The reactor is placed in a three-zone electrically heated oven, which allows an isothermal reaction zone within ±5 K of 20 cm in length and 0.87 cm of inner diameter. Reaction products are cooled at the outlet of the reactor by means of air addition through an external refrigeration jacket. The total flow rate in the experiments is around 1 L (STP)/min, which gives a temperature dependent gas residence time in the isothermal reaction zone, as stated in the experiments description, Table 1. A schematic of the set-up can be found in the Supplementary Material (Fig. SM1), together with the longitudinal temperature profiles within the reactor (Fig. SM2)

Downstream the reactor, the product gas is directed to a gas micro-chromatograph equipped with TCD detectors (Agilent Technologies) for NH_3, O_2, H_2, N_2 and N_2O quantification, and to continuous analyzers for NH_3 (infra-red), NO (infra-red), NO_2 (ultraviolet), and N_2O (infra-red), all of them from ABB Measurement and Analytics. The uncertainty of the measurements is estimated within 5%, and not less than 5 ppm for the continuous analyzers and 10 ppm for the TCD detectors [11].

Table 1 shows the conditions of the test cases. Sets 4 and 4R are repeated experiments at stoichiometric conditions, and set 5 is a third repetition but in the presence of 5000 ppm H_2O. All the experiments have been carried out with a NH_3 concentration of around 1000 ppm.

As it can be observed, experimental sets 1–11 have been performed in a nitrogen atmosphere. For around 1000 ppm of NO, the influence of λ (from 0 to 4.85) has been studied, sets 1–7. The influence of the NH_3/NO ratio has been analyzed for different λ values, λ∼1.7 (sets 8, 6, 9) and λ∼5 (sets 10, 7, 11).

Experimental sets 12–24 have been performed in an argon atmosphere. For around 1000 ppm of NO, the influence of λ (from 0.49 to 5.48) has been analyzed (sets 12–18). The influence of the NH_3/NO ratio has been studied for three different λ values: λ∼1 (sets 19, 14, 20), λ∼2.3 (sets 21, 17, 22) and λ∼5.5 (sets 23, 18, 24).

3. Chemical-kinetic modeling

Computations have been performed using the PFR model of the Chemkin Pro suite [24]. The mechanism of Glarborg et al. [25], with minor updates included in the study of CH_3CN conversion by Alzueta et al. [26], and including the interaction of NH_3 and NH_2 to produce N_2H_3 and H_2, as described in the work of Dove and Nip [27], as in the work of Abián et al. [11], has been used for simulations. This reaction mechanism includes submechanisms for C1-C2 hydrocarbons [28–30], amines [31], cyanides [32] and hydrocarbon/nitrogen interactions [33–35]. Additionally, the reaction mechanism has been extended with the recent work of Glarborg et al.

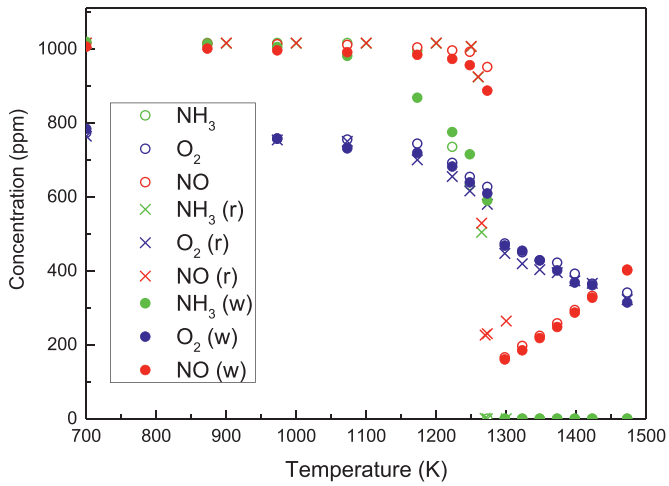

Fig. 1. Concentration of ammonia, oxygen and nitric oxide as a function of temperature for stoichiometric conditions both in the absence and presence of water vapor. Sets 4 (open circles), 4R (crosses) and 5 (solid circles) in Table 1.

[36], to account for new determined third-body collisions efficiencies in NH_2+H(+M) and NH_2+NH_2(+M) reactions. The rate constants for the reverse reactions were computed from the forward rate constants and the equilibrium constants using the thermodynamic data from the same sources as the kinetic mechanisms. The full mechanism in CHEMKIN format can be found as supplementary material.

4. Results and discussion

The study of the influence of the presence of NO, which can be formed from NH_3 in a real combustion device, during ammonia combustion is of interest, and the present work addresses the conversion of NH_3/NO mixtures for different temperatures and stoichiometries, including also fuel-rich conditions that are not usually considered in studies devoted to the Thermal $DeNO_x$ process by the use of ammonia as selective non-catalytic agent. The interaction of ammonia with nitric oxide under combustion conditions has been systematically considered in the present work by evaluating the effect of temperature, air stoichiometry, NH_3/NO ratio and the presence of water vapor for two different bulk gases (N_2 or Ar), on the conversion of both ammonia and nitric oxide and the formation of the main reaction products. As mentioned in the experimental section, the use of argon as bath gas allows the quantification of the N_2 formed and, therefore, to carry out nitrogen balances in the experiments, as it will be seen later.

Figure 1 shows an example of the conversion of ammonia and concentration of NO as a function of temperature for stoichiometric conditions, for two repeated experiments performed under stoichiometric conditions (sets 4 and 4R in Table 1). The inlet concentrations are around 1000 ppm NH_3, 1000 ppm NO and 750 ppm O_2. Additionally, Figure 1 also includes a third repetition of the same experiment, but including the presence of 5000 ppm of water (set 5 in Table 1). Figure 1 also shows the measured O_2 in the experiments, to compare as well repetitiveness with a non-nitrogen compound. The choice of 5000 ppm of water is related to the possible formation of water from ammonia in a real combustion process (1000 ppm of water would produce 1500 ppm of water) as well as the possible co-combustion of ammonia with other combustibles containing hydrogen. Additionally, this value is comparable to those used in previous works by our group (e.g. 11).

Under stoichiometric conditions, conversion of ammonia starts approximately at 1150–1200 K, originating a decrease in NO concentration at a slightly higher temperature. At a temperature

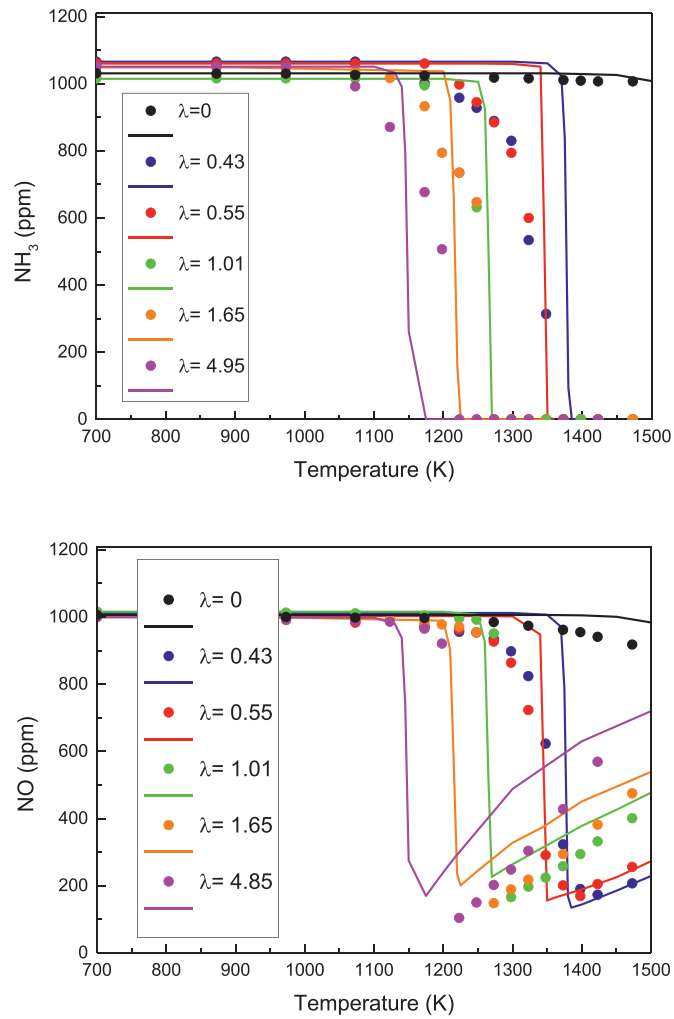

Fig. 2. Concentrations of NH_3 (a) and NO (b) as a function of temperature for different stoichiometries using N_2 as bath gas. Sets 1 (λ=0), 2 (λ=0.43), 3 (λ=0.55), 4 (λ=1.01), 6 (λ=1.65), and 7 (λ=4.85) of Table 1.

slightly above 1250 K, conversion of ammonia is seen to reach 100%. The diminution of NO proceeds in parallel with the decrease in NH_3 up to approximately 1270 K, where the maximum NO decrease is observed. Above this temperature, the NO concentration increases again monotonically. Repetitiveness of the experiments is pretty good, as shown in Fig. 1 when comparing open symbols and crosses, both when comparing the nitrogen species and the concentration of oxygen. The impact of water (solid symbols), by adding 5000 ppm H_2O, is not seen to be significant under the studied conditions, and differences observed can be attributed to the small differences in the experimental conditions of sets 4 and 4R, with no water present, and 5 with water vapor. This observation is different from the results obtained by Ariemma et al. [37] when studying ammonia combustion under mild conditions, which indicate a promoting effect of water addition for NO reduction. However, it has to be mentioned that, apart from the significantly different operating conditions and reaction system, the amounts of water vapor considered in the work of Ariemma et al. [37] were higher than 25%.

Under the present studied conditions, the NO_2 concentration is always around the detection limit (below 5 ppm). This low NO_2 concentration is attributed to the fact that at the high temperatures considered the presence of NO_2 is not thermodynamically favored compared to the NO formation. The N_2O concentration (not shown) exhibits a peak of less than 20 ppm at the temperature for

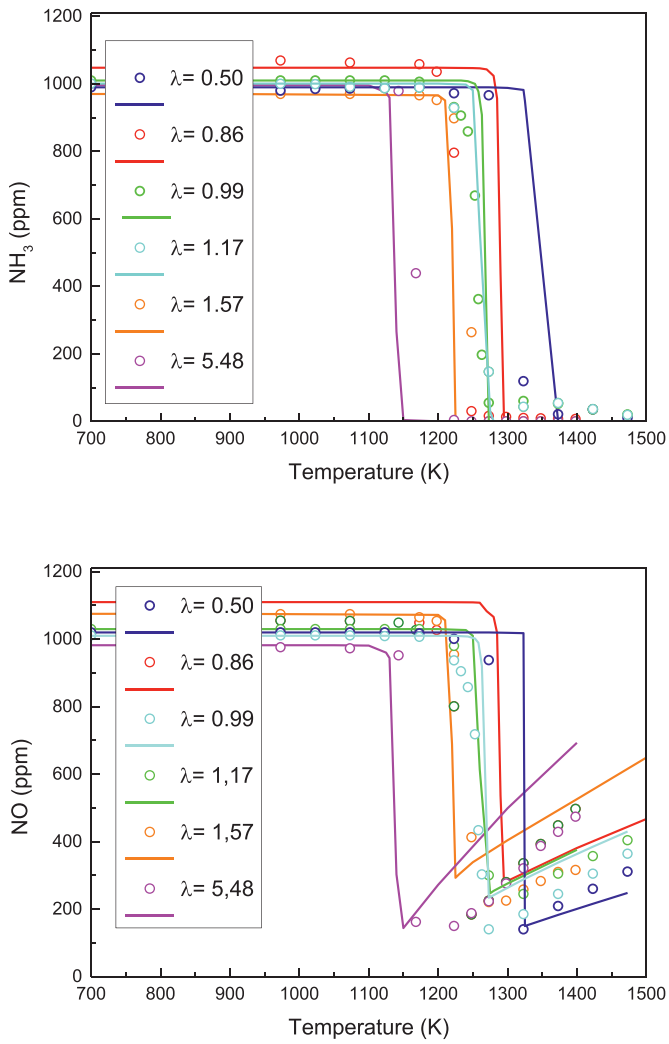

Fig. 3. Concentrations of NH_3 (a) and NO (b) as a function of temperature for different stoichiometries using Ar as bath gas. Sets 12 (λ=0.49), 13 (λ=0.86), 14 (λ=0.99), 15 (λ=1.17), 16 (λ=1.57), and 18 (λ=5.48) of Table 1.

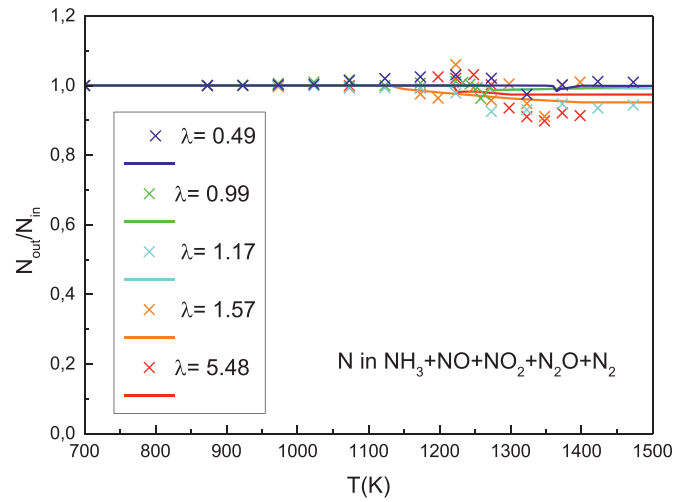

Fig. 4. Comparison between experimental and calculated results of the balance of nitrogen as a function of temperature for different stoichiometries, in the presence of argon as bath gas. Species included in the balance are NH_3, NO, NO_2, N_2O and N_2.

which the maximum conversion of ammonia is reached and the maximum reduction of NO is attained, and it is very low or none for the rest of conditions studied.

The influence of stoichiometry (from pyrolysis to very lean conditions) on NH_3 conversion and NO concentration as a function of temperature can be seen in Figs. 2 and 3, respectively for nitrogen and argon bath gas atmospheres. Symbols represent experimental results and lines correspond to model calculations. As seen in Fig. 2, conversion of ammonia is almost negligible in the absence of oxygen under the conditions considered. Only at temperatures close to 1500 K, the highest temperature studied in the present work, NH_3 is seen to exhibit a slight decay, which is captured by the model. When stoichiometry is increased, the conversion of NH_3 is shifted to lower temperatures. As mentioned above for stoichiometric conditions, also for the rest of stoichiometries considered and regardless of the fuel-rich or fuel-lean environment, at the temperature where the NH_3 concentration reaches zero, i.e. its maximum conversion, the minimum NO concentration is reached. Maximum NO conversions reached are indicated in Table 2, for the case of using N_2 as bath gas. Above the temperature for maximum NO reduction, the NO concentration increases again monotonically with the increase in temperature. It is seen in Table 2 that the maximum NO reduction that can be achieved increases as the oxygen availability in the reaction environment is higher, in agreement with the general knowledge related to the Thermal $DeNO_x$ process. This indicates that NO removal efficiency is maximum under excess oxygen conditions, where the formation of NH_2 radicals from NH_3 is maximized (e.g. [16]). These observed main features are common to both N_2 and Ar as bath gases.

Figure 3 depicts the results of selected stoichiometries (ranging from fuel-rich to fuel-lean) in an argon atmosphere, and similar behavior and observations as in Fig. 2 can be made. This was also observed in previous results by our group [38], which indicated that the influence of the bath gas is not significant for the results obtained in a study of ammonia conversion under pyrolysis conditions. Despite the fact that in industrial combustion of ammonia with air, nitrogen will be the dominant compound, the use of argon as bath gas allows the performance of a nitrogen balance. The N balance, corresponding to the experimental results of Fig. 3, is shown in Fig. 4. The N balance has been made considering the totality of the nitrogen species measured, that is: NH_3, NO, NO_2, N_2O, and N_2, both for the experimental and calculated results. The sum of N in the referred species, divided by the inlet concentration of N, is plotted in Fig. 4 as a function of temperature for different stoichiometries. As seen, both experimental and calculated results coincide reasonably well and, in both cases, the balance closes always within 90 ± 10%, indicating that the measured species in the experiments are clearly the dominant ones, in particular NO and NH_3, and the formed N_2.

Additionally, Figures 2 and 3 include the results of simulations carried out with the model reported before. In general, the model captures the main trends that are observed experimentally and the temperature windows where conversion occurs. While the NH_3 and NO profiles predicted by the model in the N_2 atmosphere are slightly sharper compared to the experimental observations, in the argon environment predictions are closer to experimental data. The reason for that different behavior is unknown at present and it may indicate a third body effect of the bath gas, affecting one or more individual reactions important for the present reacting system. This issue may deserve further investigation.

The influence of the NH_3/NO ratio has also been studied. Figure 5 shows the results of NH_3 and NO concentrations, as a function of temperature, for λ∼1.6, different NH_3/NO ratios and N_2 as bath gas (sets 8, 6, 9 in Table 1). The results corresponding to λ∼5 (sets 10, 7, 11) are presented in Fig. SM3 in the Supplemen-

Table 2
Maximum NO reduction achieved, and temperatures at which it is reached, for different stoichiometries.

	λ=0 (Set 1)	λ=0.43 (Set 2)	λ=0.55 (Set 3)	λ=1.01 (Set 4)	λ=1.65 (Set 6)	λ=4.85 (Set 7)
NO reduction (%)	8.7	82.6	83.0	83.8	85.2	89.6
Temperature for max. NO reduction (K)	1475	1400	1375	1300	1275	1225

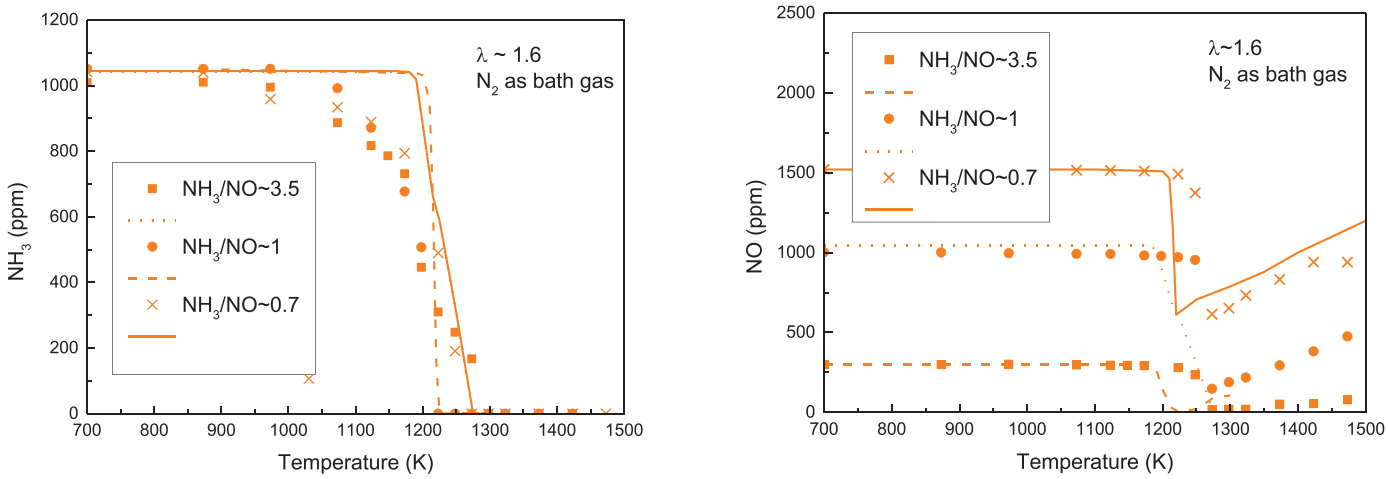

Fig. 5. NH_3 (left) and NO (right) concentrations as a function of temperature for different NH_3/NO ratios and a λ of around 1.6. N_2 as bath gas. Sets 8, 6, 9 in Table 1.

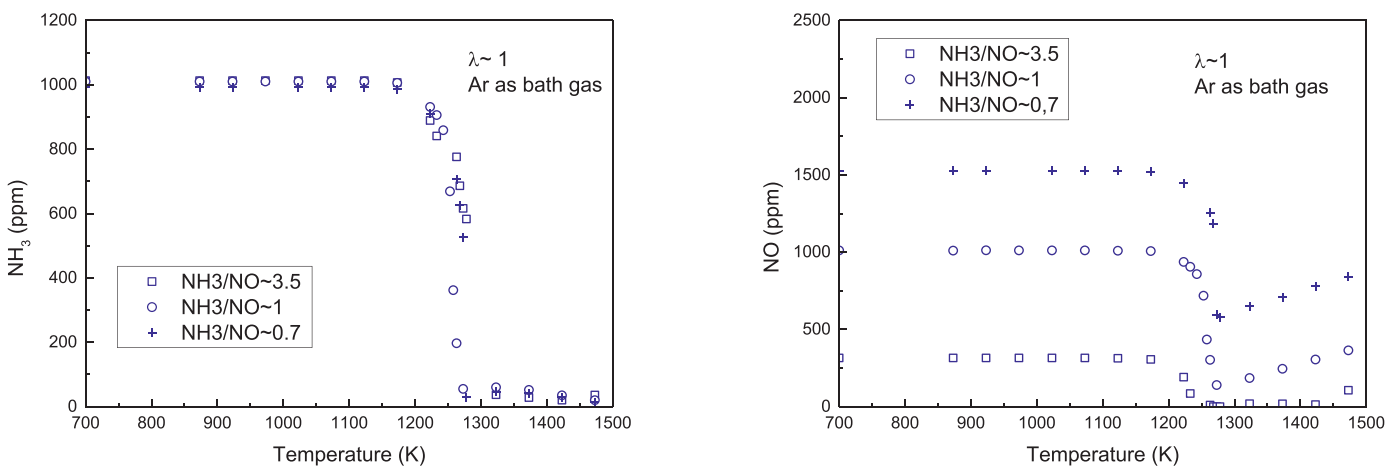

Fig. 6. NH_3 (left) and NO (right) concentrations as a function of temperature for different NH_3/NO ratios and a λ of around 1. Ar as bath gas. Sets 19, 14, 20 in Table 1.

tary Material. Figure 6 shows the NH_3 and NO concentrations, as a function of temperature, for λ∼1, different NH_3/NO ratios and Ar as bath gas (sets 19, 14, 20 in Table 1). The results corresponding to λ∼2.3 (sets 21, 17, 22 in Table 1) and to λ∼5.5 (sets 23, 18, 24 in Table 1) are presented in the Supplementary Material (Figs. SM4 and SM5).

In general, the main observations using Ar or N_2 as bath gas are similar, even though the decay of NH_3 concentration appears to be slightly sharper in the Ar atmosphere. The reason for this is unknown at present and may deserve further study, even though for practical industrial combustion conditions of only the N_2 environment is of interest.

Specifically, while the NH_3 concentration has been kept at a nominal value of 1000 ppm, NO concentration has been changed between 300 and 1500 ppm, which results in NH_3/NO ratios between approximately 3.5 and 0.7. The objective of the present experiments is to evaluate the impact if any, on the one hand, to evaluate the capacity of NH_3 to reduce NO and, on the other hand, of a possible mutual sensitization of NH_3 and NO. The present experiments have been carried out under fuel-lean conditions, since those are the most appropriate to exhibit a significant reduction of NO, by action of SNCR reactions.

Independently of the stoichiometry and the bath gas, the present results indicate that the addition of different concentrations of NO to 1000 ppm NH_3 does not have a significant effect on the NH_3 and NO conversion regimes. This fact generally agrees with the findings of Kasuya et al. [39] and Rota et al. [40], in studies of NO reduction under SNCR conditions. Those works investigated the effect of the influence of partial pressure of all the reactants, and in particular the effect of the NH_3/NO ratio on the overall NO abatement, and found little effect of the NH_3/NO ratio on the temperature window for NO reduction with a non-complete abatement of NO for NH_3/NO ratios equal or lower than 1, which agrees with the results of the present work. However, this outcome is in contrast with previous findings, by Dagaut [19], in jet-stirred reactor (JSR) experiments where the NO addition was seen to shift the temperature regime for ammonia oxidation in about 100 K to lower temperatures compared to the oxidation of net

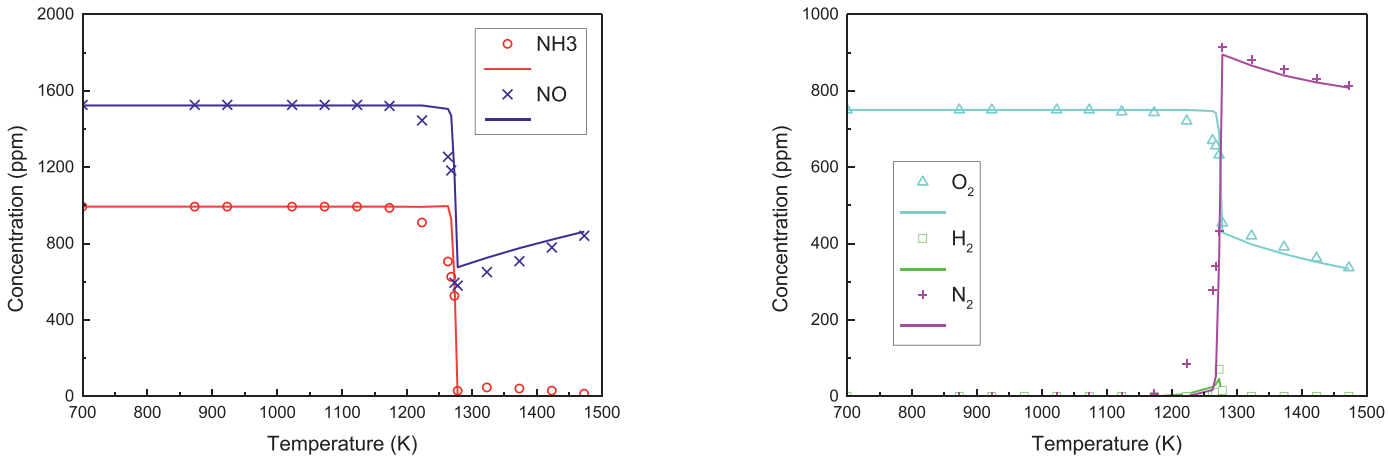

Fig. 7. Comparison between experimental and simulated results for NH_3, NO, O_2, H_2 and N_2. Set 20 of Table 1.

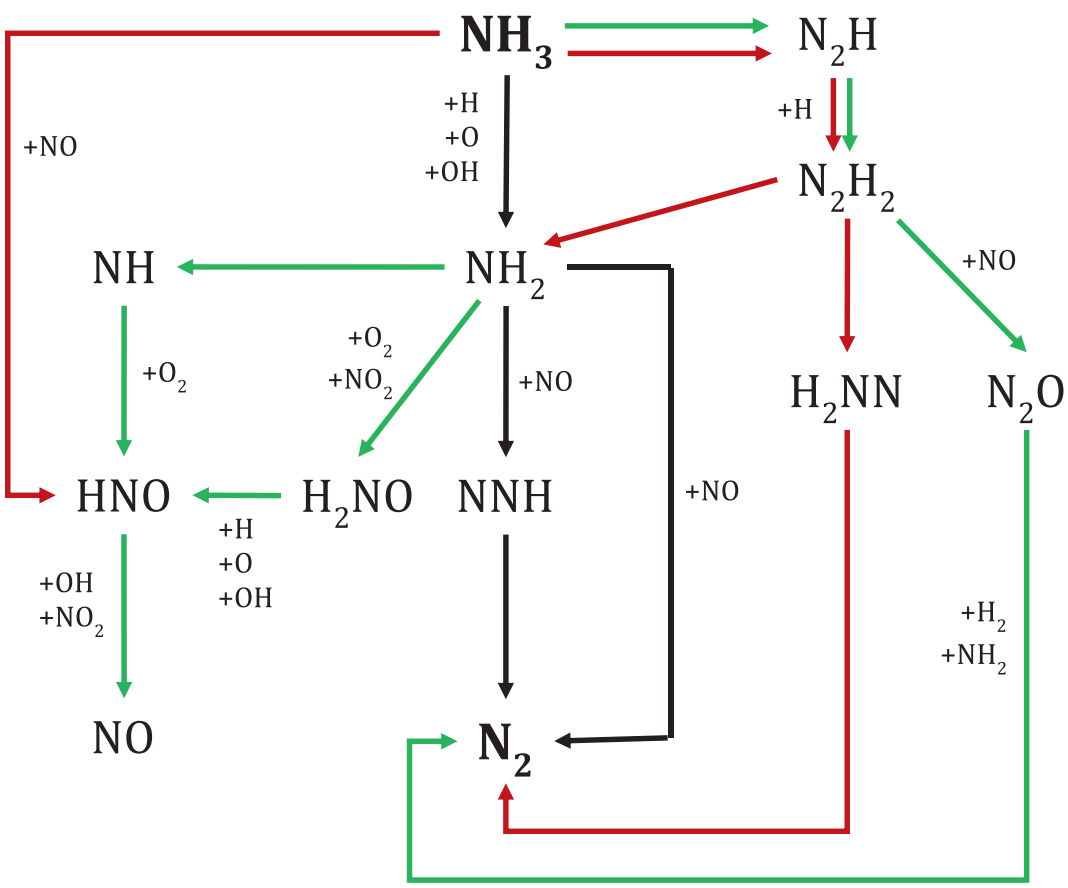

Fig. 8. Reaction path diagram for the conversion of NH_3 under the conditions of the present work. Black lines correspond to stoichiometric conditions, and red and green lines correspond respectively to fuel-rich and fuel-lean ones.

NH_3. The different behaviors of Dagaut's experiments and ours can be attributed to the different specific reactions and experimental conditions considered in both cases. In order to further explore this issue, we have done simulations for the experimental data of Dagaut's work [19] and an example is shown in Fig. SM6 in the supplementary material. Figure 5 shows additionally the computed NH_3 and NO profiles. Despite some differences in the experimental and modelling comparison in Figs. 5 and SM6, both experimental and calculated profiles appear to be globally well described, indicating the negligible effect of the addition of different amounts of NO for the conversion of ammonia, under the conditions of the present work. Similar findings are obtained for other cases, not shown. The reasonable agreement between experimental and simulated data obtained also for Dagaut's results reinforces our hypothesis of attributing differences between experimental results to the specific experimental conditions obtained in the different works.

As it has been mentioned, experiments performed using Ar as bath gas allow to quantify the N_2 formed in the reaction. As an example, Figure 7 shows the comparison between experimental results and model calculations corresponding to set 20 in Table 1. Comparison with model simulations for all the species measured

Table 3
Maximum reduction of NO achieved for the different NH_3/NO ratios for the conditions of Figs. 5 and 6.

	Maximum NO reduction (%)	
NH_3/NO ratio	N_2 atmosphere	Ar atmosphere
>1	99.0	100
~1	89.6	80.1
<1	61.2	66.1

in significant amounts in the experiment, i.e. NH_3, NO and N_2, but also O_2 and H_2, is done. As seen, despite the sharper behavior of model simulations observed at the onset of the different species conversion, the calculations reproduce well not only the nitrogen species, but also the conversion profile of oxygen, and the hydrogen and nitrogen formed.

Despite the negligible effect of NO on NH_3 conversion, an increase in the NH_3/NO ratio does result in a higher reduction of NO, which is almost total for the NH_3/NO ratio of 3.5. Table 3 shows the maximum percentage of NO reduction achieved under the conditions of Figs. 5 and 6. Despite the differences in the specific values, which can be attributed to the specific experimental conditions, it can be concluded that the interaction NH_3–NO is almost quantitative, and proceeds mole to mole. Also, similar findings are obtained for the different air stoichiometries considered and both in the presence of N_2 or Ar as bath gases.

Chemistry of ammonia conversion has been described in detail in the literature, and the main issues are known (e.g. 4–8, [11,16,25]), in particular when it proceeds at high temperatures and under oxygen excess conditions, typical for the selective non-catalytic reduction process, which has been recently further explored in the work of Stagni et al. [6]. Ammonia conversion follows two main reaction pathways, both with NH_2 radicals as main intermediates, one going through H_2NO and subsequently through HNO [6,11,25] which is dominant under fuel-lean conditions, and a second one proceeding through NNH (e.g. [16,25,41]), which is more relevant as the oxygen availability diminishes.

The reaction mechanism has been used to perform reaction pathway analysis under the conditions of the experiments, in order to delineate the main reaction routes through which the conversion of NH_3 and NO proceeds during the conversion of the NH_3/NO mixtures. Figures 8 and 9 show respectively the main pathways for NH_3 and NO conversion at different stoichiometries and at the temperature of the onset for NO conversion, i.e. when the interaction NH_3/NO starts.

Calculations made with the present mechanism indicate that the main reaction pathways for ammonia conversion in the presence of NO are very similar to those happening in the absence of this contaminant, as shown in our recent study of ammonia oxidation [11], with a clear predominancy of the $NH_3 \rightarrow NH_2 \rightarrow NNH \rightarrow N_2$ pathway compared to the case with no NO present. This is explained because once the NH_2 radicals are formed, they compete for NO and the radical pool constituents. Since both the concentration of NO is comparatively high and the NH_2/NO reaction is pretty fast, reactions

$$NH_2 + NO \rightleftharpoons N_2 + H_2O \quad \text{(r2)}$$

and

$$NH_2 + NO \rightleftharpoons NNH + OH \quad \text{(r4)}$$

followed by decomposition of NNH into N_2, are the main paths for NH_3 and NO decrease, being responsible of the reduction of NO under all the conditions of the present work.

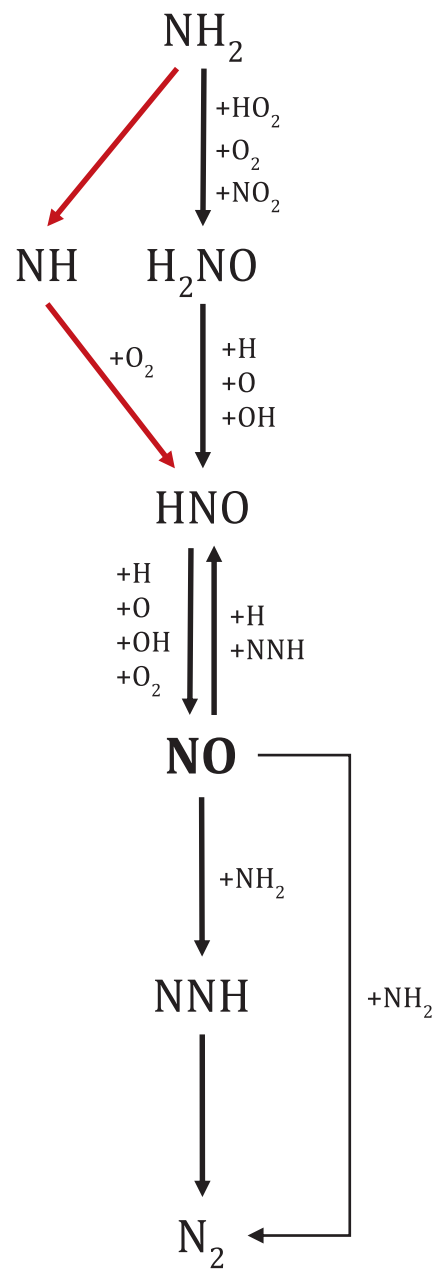

Fig. 9. Reaction path diagram for the conversion of NO under the conditions of the present work. . Black lines correspond to stoichiometric and fuel-lean conditions, and red lines correspond respectively to fuel-rich ones.

Additionally, under fuel-lean conditions, additional reaction paths leading to the reduction of NO are activated, mainly one proceeding through N_2O, reaction sequence r5-r8:

$$NH_3 + NH_2 \rightleftharpoons N_2H_3 + H_2 \quad \text{(r5)}$$

$$N_2H_3 + H \rightleftharpoons N_2H_2 + H_2 \quad \text{(r6)}$$

$$N_2H_2 + NO \rightleftharpoons NH_2 + N_2O \quad \text{(r7)}$$

$$N_2O + M \rightleftharpoons N_2 + O + M \quad \text{(r8)}$$

which is responsible for the experimental observation of few ppm of N_2O, and a second one, proceeding through H_2NO, which finally recycles HNO into NO (reaction sequences r9-r16),

$$NH_2 + O_2 \rightleftharpoons H_2NO + O \quad \text{(r9)}$$

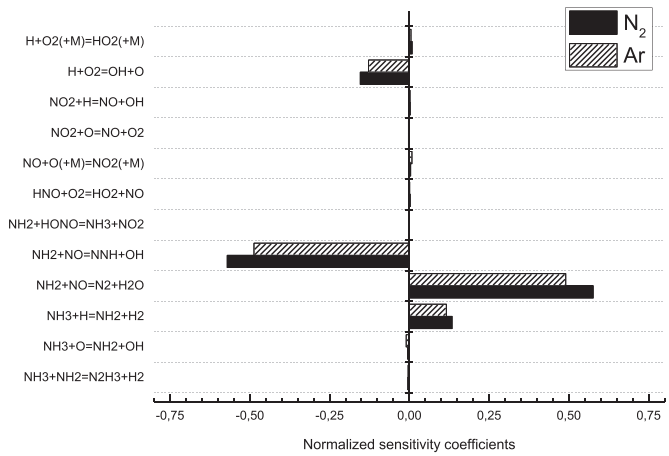

Fig. 10. Sensitivity analysis for NH_3 conversion for experiments carried out under stoichiometric conditions with N_2 (Set 4 of Table 1, 1250 K) or Ar (set 14 of Table 1, 1255 K) as diluents.

H_2NO has been pointed out as an important intermediate species during NH_3 conversion [11, 25]. Once formed, H_2NO produces quantitatively the HNO species, which reacts to produce NO, i.e.:

$$H_2NO+H/O/OH \rightleftharpoons HNO+H_2/OH/H_2O \quad \text{(r10–12)}$$

$$HNO+H/O/OH/O_2 \rightleftharpoons NO+H_2/OH/H_2O/HO_2 \quad \text{(r13–16)}$$

Normalized sensitivity coefficients for NH_3 concentration for the conditions of sets 4 ($\lambda = 1.01$) with N_2 as diluent and 14 ($\lambda = 0.99$) with Ar as diluent in Table 1 are shown in Fig. 10. No significant differences are found for the most sensitive reactions in either N_2 or Ar as diluents, and therefore no insight on the observed differences between fitting of the calculations with experimental results can be drown at present. The senstitivity analysis also shows that the main reactions driving the reactivity of ammonia involve the formation of NH_2 radicals, which mainly interact with NO.

5. Conclusions

An experimental and simulation study of the interaction of NH_3 and NO under a wide range of operating conditions has been performed in a quartz tubular flow reactor set-up, at atmospheric pressure and in the 700–1500 K temperature range. Different air stoichiometries, from very fuel-rich to very fuel-lean, were considered ($\lambda = 0$ to 5). The impact of the NH_3/NO ratio was evaluated, using values from 0.7 to 3.5. Experiments were performed both in nitrogen and argon atmospheres. The results of the tests performed were interpreted in term of a literature detailed chemical-kinetic mechanism.

Results obtained have allowed to determine the extent of the interaction between NH_3 and NO under a variety of air stoichiometries, as a function of temperature, including also fuel-rich conditions, which have been scarcely considered in the literature. Results indicate that the reduction of NO is produced at almost any stoichiometry, even though fuel-lean environments are the most appropriate for NO reduction, as the general knowledge of the thermal deNO_x process indicates. Calculations show that reduction of NO by ammonia is produced by interaction with NH_2 radicals under any stoichiometry conditions, while as the oxygen availability increases, additional paths going through N_2O are activated, increasing thus the reduction of NO under those excess oxygen conditions. Additionally, it is seen that the oxygen availability determines the temperature window at which both conversion of ammonia and reduction of NO occur.

No significant sensitization effects have been observed when using different NH_3/NO ratios in the experiments. The interaction between NH_3 and NO proceeds in a molar basis, with very high conversions of NO (almost 100%) under optimum conditions. In general, similar findings have been obtained using N_2 or Ar as bath gases.

The literature mechanism used for simulating the experimental results does reflect the main trends experimentally observed and has been used to determine the main reaction pathways through which the interaction of NH_3 and NO proceed. The main interaction occurs through the NH_2+NO reaction mechanism, under any stoichiometry. As the oxygen availability is higher, the reduction of NO by action of ammonia is higher as well, because also reaction paths going through the N_2O species appear to be significant.

Declaration of Competing Interest

None.

Acknowledgments

The authors express their gratitude to the Aragón Government (Ref. T22_20R), co-funded by FEDER 2014–2020 "Construyendo Europa desde Aragón", and to MCIU and FEDER (Project RTI2018–098856-B-I00) for financial support.

Supplementary materials

Supplementary material associated with this article can be found, in the online version, at doi:10.1016/j.combustflame.2021.111691.

References

1. H. Kobayashi, A. Hayakawa, K.D.K.A. Somarathne, E.C. Okafor, Science and technology of ammonia combustion, Proc. Combust. Inst. 37 (2019) 109–133.
2. A. Valera-Medina, H. Xiao, M. Owen-Jones, W.I.F. David, P.J Bowen, Ammonia for power, Prog. Energy Combust. Sci. 69 (2018) 63–102.
3. B. Shu, S.K. Vallabhuni, X. He, G. Issayev, K. Moshammer, A. Farooq, R.X. Fernandes, A shock tube and modeling study on the autoignition properties of ammonia at intermediate temperatures, Proc. Combust. Inst. 37 (2019) 205–211.
4. O. Mathieu, E.L Petersen, Experimental and modeling study on the high-temperature oxidation of ammonia and related NO_x chemistry, Combust. Flame 162 (2015) 554–570.
5. M.V. Manna, P. Sabia, R. Ragucci, M. de Joannon, Oxidation and pyrolysis of ammonia mixtures in model reactors, Fuel 264 (2020) 116768.
6. A. Stagni, C. Cavalloti, S. Arunthanayothin, Y. Song, O. Herbinet, F. Battin-Leclerc, T. Faravelli, An experimental, theoretical and kinetic-modeling study of the gas-phase oxidation of ammonia, React. Chem. Eng. 5 (2020) 696–711.
7. Y. Song, H. Hashemi, J.M. Christensen, C. Zhou, P. Marshall, P. Glarborg, Ammonia oxidation at high pressure and intermediate temperatures, Fuel 181 (2016) 358–365.
8. K.P. Shrestha, L. Seidel, T. Zeuch, F Mauss, Detailed kinetic mechanism for the oxidation of ammonia including the formation and reduction of nitrogen oxides, Energy Fuel 32 (2018) 10202–10217.
9. O. Elishav, B.M. Lis, E.M. Miller, D.J. Arent, A. Valera-Medina, A.G. Dana, G.E. Shter, G.S. Grader, Progress and prospective of nitrogen-based alternative fuels, Chem. Rev. 120 (2020) 5352–5436.
10. A. Valera-Medina, F. Amer-Hatem, A.K. Azad, I.C. Dedoussi, M. de Joannon, R.X. Fernandes, P. Glarborg, H. Hashemi, X. He, S. Mashruk, J. McGowan, C. Mounaim-Rouselle, A. Ortiz-Prado, A. Ortiz-Valera, I. Rossetti, B. Shu, M. Yehia, H. Xiao, M. Costa, Review on ammonia as a potential fuel: from synthesis to economics, Energy Fuel 35 (2021) 6964–7029.
11. M. Abián, M. Benés, A. de Goñi, B. Muñoz, M.U. Alzueta, Study of the oxidation of ammonia in a flow reactor. Experiments and kinetic modeling simulation, Fuel 300 (2021) 120979.
12. M. Barbas, M. Costa. S. Vranckx, R.X. Fernandes, Experimental and chemical kinetic study of CO and NO formation in oxy-methane premixed laminar flames doped with NH_3, Combust. Flame 162 (2015) 1294–1303.
13. R. Cavaliere da Rocha, M. Costa, X.S. Bai, Chemical kinetic modelling of ammonia/hydrogen/air ignition, premixed flame propagation and NO emission, Fuel 246 (2019) 24–33.

14. P. Dagaut, A. Nicolle, Experimental and kinetic modeling study of the effect of SO_2 on the reduction of NO by ammonia, Proc. Combust. Inst. 30 (2005) 1211–1218.
15. C.C. Schmidt, C.T. Bowman, Flow reactor study of the effect of pressure on the thermal De-NO_x process, Combust. Flame 127 (2001) 1958–1970.
16. J.A. Miller, P. Glarborg, Modeling the thermal De-NO_x process: closing in on a final solution, Prog. Energy Combust. Sci. 15 (1989) 287–338.
17. M.U. Alzueta, H. Røjel, P.G. Kristensen, P. Glarborg, K. Dam-Johansen, Laboratory study of the $CO/NH_3/NO/O_2$ system. Implications for hybrid reburn/SNCR strategies, Energy Fuel 11 (1997) 716–723.
18. B. Mei, J. Zhang, X.X. Shi, Z. Xi, Y. Li, Enhancement of ammonia combustion with partial fuel cracking strategy: laminar flame propagation and kinetic modeling investigation of $NH_3/H_2/N_2$/air mixtures up to 10 atm, Combust. Flame 231 (2021) 111472.
19. P. Dagaut, Mutual sensitization of the oxidation of NO and ammonia: experimental and kinetic modeling, 11th Mediterranean Combustion Symposium, Combustion Institute, 2019 hal-02271596.
20. M.U. Alzueta, R. Bilbao, M. Finestra, Methanol oxidation and its interaction with nitric oxide, Energy Fuel 15 (2001) 724–729.
21. M. Abián, J. Giménez-López, R. Bilbao, M.U. Alzueta, Effect of different concentration levels of CO_2 and H_2O on the oxidation of CO: experiments and modeling, Proc. Combust. Inst. 33 (2011) 317–323.
22. M.U. Alzueta, R. Pernía, M. Abián, A. Millera, R. Bilbao, CH_3SH conversion in a tubular flow reactor: experiments and kinetic modeling, Combust. Flame 203 (2019) 23–30.
23. M.U. Alzueta, P. Glarborg, K. Dam-Johansen, Low temperature interactions between hydrocarbons and nitric oxide: an experimental study, Combust. Flame 109 (1997) 25–36.
24. , ANSYS Chemkin, 18, ANSYS Inc, 2016.
25. P. Glarborg, J.A. Miller, B. Ruscic, S.J. Klippenstein, Modeling nitrogen chemistry in combustion, Prog. Energy Combust. Sci. 57 (2018) 31–68.
26. M.U. Alzueta, M. Guerrero, A. Millera, P. Marshall, P. Glarborg, Experimental and kinetic modeling study of oxidation of acetonitrile, Proc. Combust. Inst. 38 (2021) 575–583.
27. J.E. Dove, W.S. Nip, Shock-tube study of ammonia pyrolysis, Can. J. Chem. 57 (1979) 689–701.
28. H. Hashemi, J.M. Christensen, S. Gersen, H. Levinsky, S.J. Klippenstein, P. Glarborg, High-pressure oxidation of methane, Combust. Flame 172 (2016) 349–364.
29. H. Hashemi, J.G. Jacobsen, C.T. Rasmussen, J.M. Christensen, P. Glarborg, S. Gersen, M. van Essen, H. Levinsky, S.J. Klippenstein, High-pressure oxidation of ethane, Combust. Flame 182 (2017) 150–166.
30. J. Giménez-López, C.T. Rasmussen, H. Hashemi, M.U. Alzueta, Y. Gao, P. Marshall, C.F. Goldsmith, P. Glarborg, Experimental and kinetic modeling study of C_2H_2 oxidation at high pressure, Int. J. Chem. Kinet. 48 (2016) 724–738.
31. S.J. Klippenstein, L.B. Harding, P. Glarborg, J.A. Miller, The role of NNH in NO formation and control, Combust. Flame 158 (2011) 774–789.
32. P. Dagaut, P. Glarborg, M.U. Alzueta, The oxidation of hydrogen cyanide and related chemistry, Prog. Energy Combust. Sci. 34 (2008) 1–46.
33. P. Glarborg P, M.U. Alzueta, K. Dam-Johansen, J.A. Miller, Kinetic modeling of hydrocarbon/nitric oxide interactions in a flow reactor, Combust. Flame 115 (1998) 1–27.
34. T. Mendiara, P. Glarborg, Ammonia chemistry in oxy-fuel combustion of methane, Combust. Flame 156 (2009) 1937–1949.
35. T. Mendiara, P. Glarborg, NO reduction in oxy-fuel combustion of methane, Energy Fuel 23 (2009) 3565–3572.
36. P. Glarborg, H. Hashemi, S. Cheskis, A.W. Jasper, On the rate constant for $NH_2+ HO_2$ and third-body collision efficiencies for NH_2+ H (+M) and $NH_2+ NH_2$ (+M), J. Phys. Chem. A 125 (2021) 1505–1516.
37. G.B. Ariemma, P. Sabia, G. Sorrentino, P. Bozza, M. de Joannon, R. Ragucci, Influence of water addition on MILD ammonia combustion performances and emissions, Proc. Combust. Inst. 38 (2021) 5147–5154.
38. M. Benés, G. Pozo, M. Abián, A. Millera, R. Bilbao, M.U. Alzueta, Experimental study of the pyrolysis of NH_3 under flow reactor conditions, Energy Fuel 35 (2021) 7193–7200.
39. F. Kasuya, P. Glarborg, J.E. Johson, K. Dam-Johansen, The thermal $DeNO_x$ process: influence of partial pressures and temperature, Chem. Eng. Sci. 50 (1995) 1455–1466.
40. R. Rota, E.F. Zanoelo, D. Antos, M. Morbidelli, S. Carrà, Analysis of the thermal $DeNO_x$ process at high partial pressure of reactants, Chem. Eng. Sci. 55 (2000) 1041–1051.
41. S.J. Klippenstein, M. Pfeifle, A.W. Jasper, P. Glarborg, Theory and modeling of relevance to prompt-NO formation at high pressure, Combust. Flame 195 (2018) 3–17.